

## Hydrogenation of Pyridine over Ni-W/Al<sub>2</sub>O<sub>3</sub> Catalyst

J. A. ANABTAWI, R. S. MANN, AND K. C. KHULBE

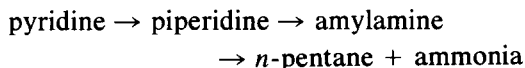
*Chemical Engineering Department, University of Ottawa, Ottawa, Canada*

Received April 4, 1979; revised December 19, 1979

The vapor-phase hydrogenation of pyridine was investigated in an integral flow reactor over Ni-W/Al<sub>2</sub>O<sub>3</sub> catalyst. The effects of various parameters, viz., temperature, initial partial pressures of the reactants, and reciprocal of space velocity, were studied. The kinetics of the hydrogenation of pyridine to form piperidine have been investigated. A rate equation for pyridine hydrogenation was derived. The activation energy was found to be 13.69 kcal/mole. A plausible mechanism has been discussed.

### 1. INTRODUCTION

Hydrogenation and hydrorefining are essential steps in upgrading crude oil. Nitrogen-and-sulfur-containing compounds are known for their basic nature, and their presence in the feed stock could neutralize the acidic sites in the hydrocracking catalyst. Most of the nitrogen is in the form of heterocyclic compounds such as indoles, quoline, and pyridine which are most resistant to hydrodenitrication (HDN). Cox (1) studied the hydrogenation of pyridine and some of its derivatives and found that the reaction was first order in pyridine and that the reaction order increased with nitrogen concentration in the feed. The kinetics of pyridine hydrogenation in paraffin oil have been recently investigated by Aboul-Gheit *et al.* (2), who reported that the reaction occurred in the following sequence:



and the rate was favored in increasing pressures.

In the present study we observed the formation of *n*-pentyl piperidine as an intermediate product. Sonnemans *et al.* (3, 4) also observed *n*-pentyl piperidine formation in the pyridine hydrogenolysis on molybdenum-containing catalysts. Goudriaan (5)

observed substantial concentration of *n*-pentyl piperidine in the products during hydrodenitrogenation of pyridine.

McIlvried (6) studied HDN of pyridine over Ni-Co-Mo/Al<sub>2</sub>O<sub>3</sub> catalyst. He observed that the apparent rate constant decreases with increasing nitrogen content and suggested that nitrogen compounds are strongly adsorbed on the catalyst. He also suggested a Langmuir-Hinshelwood type kinetic model from the data obtained during denitrication of piperidine. Satterfield *et al.* (7) studied the interaction between hydrodesulfurization (HDS) of thiophene and the HDN of pyridine. At lower temperatures, thiophene inhibited the HDN reaction. A two-site mechanism was proposed to explain this behavior (7). Sonnemans *et al.* (3, 8) studied the hydrogenation of pyridine over Mo/Al<sub>2</sub>O<sub>3</sub> and Co-Mo/Al<sub>2</sub>O<sub>3</sub> catalyst and observed the reaction to be first order with respect to pyridine. Recently Gupta *et al.* (9) studied the HDN of pyridine over Co-Mo/Al<sub>2</sub>O<sub>3</sub> catalyst and reported that the overall HDN reaction proceeds through three main reactions: saturation of double bonds resulting in stoichiometric conversion of pyridine to piperidine, ring rupture to give pentylamine, and disproportionation to give *n*-pentane and ammonia.

Nickel-tungsten-alumina (7, 10, 11) catalyst is widely used in hydrodesulfurization

hydrocracking and hydrodenitrication processes. In the present paper the kinetics of the hydrogenation of pyridine over a Ni-W-alumina catalyst using an isothermal integral flow reactor are reported, including the effect of various parameters, viz., temperature, initial partial pressures of reactants, and reciprocal of space velocity, on this reaction.

## 2. CATALYST AND REACTANTS

The catalyst used in the present study was obtained from Harshaw Chemical Company. The catalyst (Ni-4303) had been prepared by impregnating Ni and W onto a  $\gamma$ - $\text{Al}_2\text{O}_3$  support (6 wt% of Ni and 19 wt% of W). The surface area was about 200  $\text{m}^2/\text{g}$  and spectrographic analysis showed that it contained traces of Co, Ti, and Cu as impurities. The  $\frac{1}{8}$ -in. extrudate catalyst was crushed and only 20 to 60-mesh size was used. The catalyst was activated by heating it in the reactor for 48 hr at 450°C in 60  $\text{cm}^3/\text{min}$  of hydrogen. Thereafter, it was conditioned for 4–5 days with pyridine and hydrogen at 150°C. At the start of the conditioning period, there was a sharp drop in the activity, which stabilized after 4–5 days. Thereafter, no change in the activity was observed for about 10 weeks of continuous use.

Fisher certified grade pyridine (sulfate less than 3 ppm, ammonia less than 10 ppm) was used. Hydrogen and helium rated at 99.95% minimum purity were used. *n*-Pentyl piperidine was prepared in our laboratory from piperidine and pentylbromide as described by Magnusson and Schierz (12). The product was 98% pure.

## 3. EQUIPMENT AND ANALYSIS

### 3.1 Equipment

The equipment and experimental procedure were essentially the same as described by Gupta *et al.* (9).

### 3.2 Analysis

The products were analyzed by Gow-Mac W-2X hot wire, 333 mount, made of

rhenium and tungsten in a temperature-regulated 4-element macrocell (Model TR-III-AWX). The detector temperature was controlled by a Fenwell Thermo switch. dc current was supplied by Gow-Mac (Model 405-C) solid-state dc power supply. Two columns (5 m long, 4 mm i.d.) arranged in parallel were packed with Chromasorb W (60–80 mesh), acid washed, and coated with 1% NaOH and 10% Carbowax 1000. The flow rate of the carrier gas (He) was 80  $\text{cm}^3/\text{min}$ , and the column temperature was programmed from 40 to 120°C at the rate of 20°C/min. While at lower temperature *n*-pentane and ammonia were separated, the higher temperature facilitated the elution of the heavier compounds, i.e., pyridine, piperidine, dipentylamine, and *n*-pentyl piperidine.

## 4. RESULTS AND DISCUSSION

Experimental data were obtained by using an isothermal integral flow reactor. The steady state was not only realized from the operating conditions, but also from the product analysis. The effects of various variables, namely, initial partial pressures of pyridine ( $p_{py}^0$ ), reaction temperature ( $T$ ), and the reciprocal of space velocity ( $W/F$ ), on the conversion of pyridine ( $X$ ) have been studied. The conversion has been defined as the ratio of moles of pyridine reacted per hour to the moles of pyridine fed per hour into the reactor. No reaction occurred between pyridine and hydrogen in the absence of the catalyst up to 450°C.

### 4.1 Effect of Temperature

The hydrogenation of pyridine was achieved by studying the effect of temperature in the range 120–380°C. The amounts of various products formed at various temperatures for a  $W/F = 3.64$  g.cat-hr/g.mole, a pressure of  $2.928 \times 10^6$  N/m<sup>2</sup>, and initial partial pressures of pyridine 9.76  $\times 10^4$ , 7.14  $\times 10^4$ , 4.8  $\times 10^4$ , and 3.61  $\times 10^4$  N/m<sup>2</sup> have been studied. Figure 1 shows the product distribution of pyridine hydrogenation at an initial partial pressure of 9.76

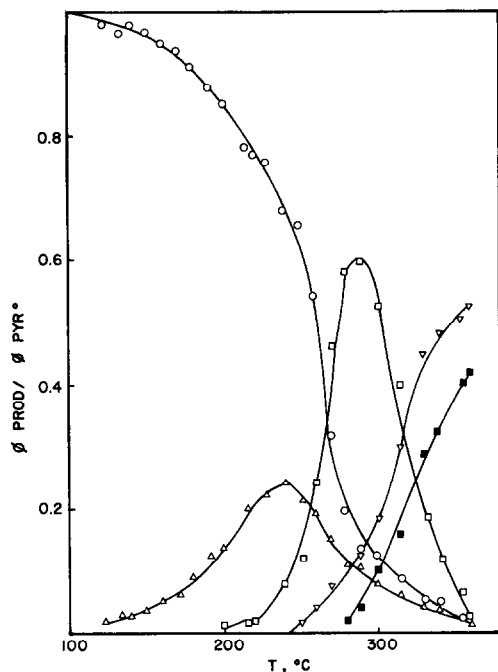
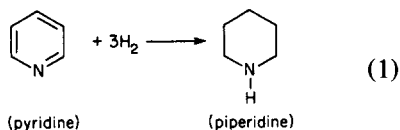


FIG. 1. Effect of temperature on product distribution at  $[p_{py}^0] = 9.76 \times 10^4 \text{ N/m}^2$ ,  $W/F = 3.64 \text{ g.cat-hr/g.mole}$ , and a total pressure of 410 psig.  $\circ$ , pyridine;  $\Delta$ , piperidine;  $\square$ , *n*-pentyl piperidine;  $\nabla$ , ammonia;  $\blacksquare$ , pentane.

$\times 10^4 \text{ N/m}^2$ . As the temperature increased, intermediate product *n*-pentyl piperidine was formed. While the concentration of *n*-pentyl piperidine decreased with the increase of temperature, the concentration of ammonia and *n*-pentane increased. At lower values of  $\bar{R}$ , other products such as *n*-pentylamine, dipentylamine, and decane formed in traces. From Fig. 1 it seems that the pyridine hydrogenation takes place in three separate reaction steps:

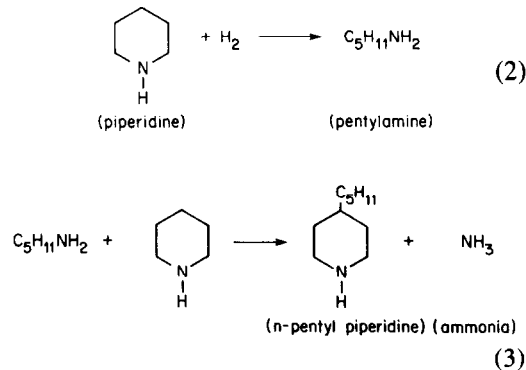
(i) Saturation of the double bonds to piperidine:



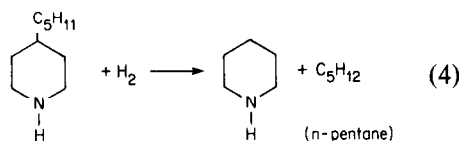
Step (1) is irreversible under experimental conditions (3, 8). Calculations showed that pyridine–piperidine equilibrium was not established in the present study under experi-

mental conditions. Several investigators (3, 5, 7) have proved that equilibrium shifts to the formation of piperidine at higher pressures and temperatures.

(ii) Above 200°C the *n*-pentyl piperidine is formed as follows:



(iii) *n*-Pentane formed from the 1-pentyl piperidine in the following way:



Reaction (2) is irreversible because the pentylamine formed immediately reacts with another molecule of piperidine giving *n*-pentyl piperidine and ammonia. Gupta *et al.* (9) observed a measurable amount of pentylamine between 120 and 180°C on Co–Mo/Al<sub>2</sub>O<sub>3</sub> catalyst. In the present study we did not get pentylamine under experimental conditions.

#### 4.2. Effect of *W/F* Ratios on the Conversion of Pyridine

The effect of the reciprocal of space velocity (*W/F*) on the conversion of pyridine was investigated in the range of *W/F* = 2.09 to 9.45 g.cat-hr/g.mole at a temperature range 145 to 280°C. Figure 2 shows the effect of *W/F* on conversion at various values of initial partial pressures of pyridine at 145°C. The conversion increased linearly with the increase of *W/F*.

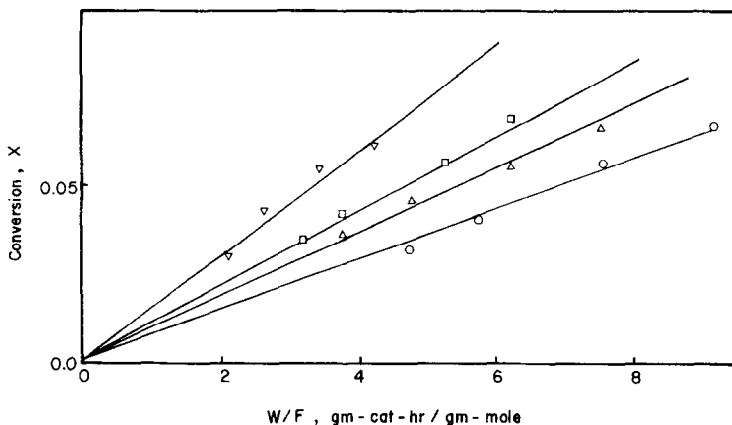


FIG. 2. Effect of  $W/F$  on conversion of pyridine at  $145^{\circ}\text{C}$  for various  $[p_{\text{py}}^0]$ :  $\circ$ ,  $7.14 \times 10^{-4}$ ;  $\triangle$ ,  $5.74 \times 10^{-4}$ ;  $\square$ ,  $4.8 \times 10^{-4}$ ;  $\nabla$ ,  $3.2 \times 10^{-4}$   $\text{N/m}^2$ .

#### 4.3. Effect of Molar Ratio of Reactants ( $\bar{R}$ )

The effect of  $\bar{R}$  at different temperatures on the conversion of pyridine was studied. Figure 3 shows the effect of  $\bar{R}$  on the conversion at a temperature range  $140$ – $220^{\circ}\text{C}$  and a  $W/F$  ratio of  $3.64$   $\text{g.cat-hr/g.mole}$ . From Fig. 3 it seems that conversion increased linearly with the increase of  $\bar{R}$ .

#### 4.4. Kinetic Analysis of Data and Rate Equation

The rate-controlling steps of a vapor-phase solid-catalyzed reaction may be the

mass transfer of the reactant or products, adsorption of reactants, desorption of reaction products, or the reaction between the adsorbed molecules on the catalyst surface. In this study, the internal and external diffusional effects were kept as low as possible by using high gas velocities and small-particle-size catalyst. The internal diffusion was determined by varying the particle size of the catalyst from  $20$ – $40$  to  $60$ – $80$  mesh keeping the temperature, residence time, and partial pressures of reactants constant. The temperature and partial pressure gradients between the flowing fluid and the exterior of the catalyst surface were evaluated by the method of Yoshida *et al.* (13).

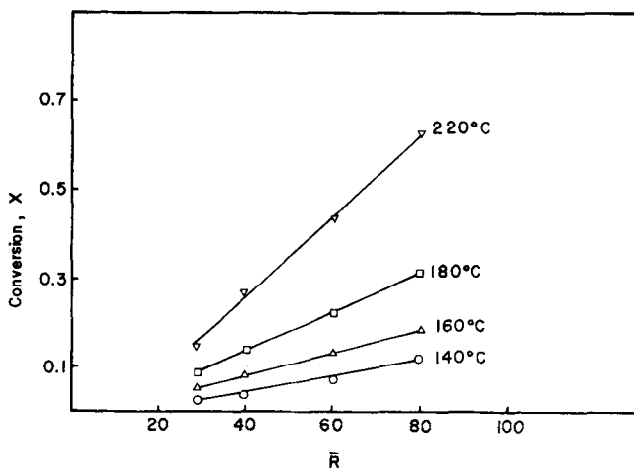


FIG. 3. Effect of molar ratio of reactant,  $\bar{R}$ , on conversion at various temperatures.

The maximum temperature difference across the film (on the catalyst surface) thus calculated was 0.1°C and the maximum partial pressure gradient was 0.001 atm, which showed that the heat and mass transfer effect were negligible.

In order to derive a rate equation for the hydrogenation of pyridine, the chemical reaction was assumed to take place as follows:



The rate equations were subsequently tested by curve fitting. Rate equations derived by McIlvried (6), Sonnemans *et al.* (3, 8), and Cox (1) were tested with the present data, but the present data did not satisfy those rate equations. The following rate equation provides the best fit for the present study:

$$r = - \frac{d[p_{py}]}{dt} = k_{ov}[p_{py}][p_{H_2}]. \quad (5)$$

Substituting

$$[p_{py}] = [p_{py}^0](1 - x)$$

and

$$[p_{H_2}] = [p_{py}^0](\bar{R} - 3x),$$

the equation will be

$$r = [p_{py}^0] \frac{dx}{dt} = k_{ov}[p_{py}^0]^2(1 - x)(\bar{R} - 3x). \quad (6)$$

By rearranging Eq. (6) we have

$$\frac{dx}{(1 - x)(\bar{R} - 3x)} = k_{ov}[p_{py}^0]dt. \quad (7)$$

By integrating Eq. (7) we have

$$\ln \left\{ \frac{\bar{R} - 3x}{\bar{R}(1 - x)} \right\} = k_{ov}[p_{py}^0](\bar{R} - 3)t = k_{ov}[p_{py}^0](\bar{R} - 3)(W/F). \quad (8)$$

A plot of  $\ln \{(\bar{R} - 3x)/\bar{R}(1 - x)\}$  against  $W/F$  should give a straight line. Figure 4 represents  $\ln \{(\bar{R} - 3x)/\bar{R}(1 - x)\}$  vs  $W/F$  for temperature 280°C. The slope of these lines give the value  $k_{ov}[p_{py}^0](\bar{R} - 3)$ . The

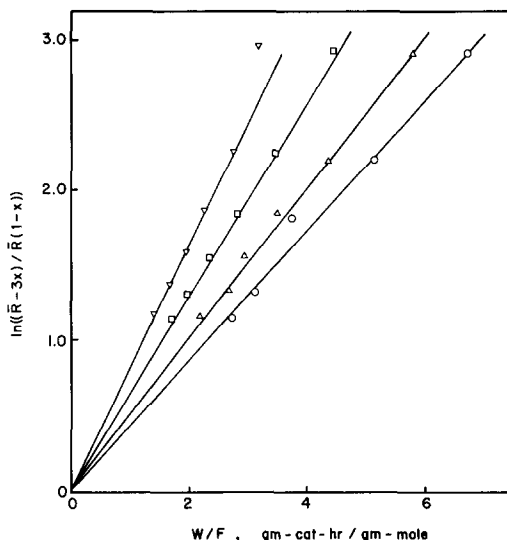


FIG. 4. Test of the rate equation (8).  $\ln((\bar{R} - 3X)/\bar{R}(1 - X))$  vs  $W/F$ .  $[p_{py}^0]$ :  $\circ$ ,  $7.14 \times 10^4$ ;  $\triangle$ ,  $5.74 \times 10^4$ ;  $\square$ ,  $4.8 \times 10^4$ ;  $\nabla$ ,  $3.2 \times 10^4$  N/m<sup>2</sup>.

rate constants were calculated from these slopes at different molar ratios.

It was observed that the  $k_{ov}$  calculated was dependent on the initial partial pressure of pyridine and could be represented as follows:

$$k_{ov} = k_s/[p_{py}^0] + k_i. \quad (9)$$

$k_s$  and  $k_i$  are functions of temperature and obtained by plotting  $k_{ov}$  against  $1/[p_{py}^0]$  at temperatures 145, 195, 245, and 280°C (Fig. 5). Values of  $k_s$  and  $k_i$  are given in Table 1.

The overall rate constant  $k_{ov}$  was assumed to be constant at a constant initial partial pressure of pyridine. The plot of  $\ln k_{ov}$  vs  $1/T$  gave a straight line satisfying the Arrhenius equation (Fig. 6). The average activation energy was found to be 13.69 kcal/mole. The final rate equation for the hydrogenation of pyridine can be written as follows:

$$r = - \frac{d[p_{py}]}{dt} = \left( \frac{k_s}{[p_{py}^0]} + k_i \right) (p_{py})(p_{H_2}). \quad (10)$$

## 5. CONCLUSIONS

The hydrogenation of pyridine over Ni-

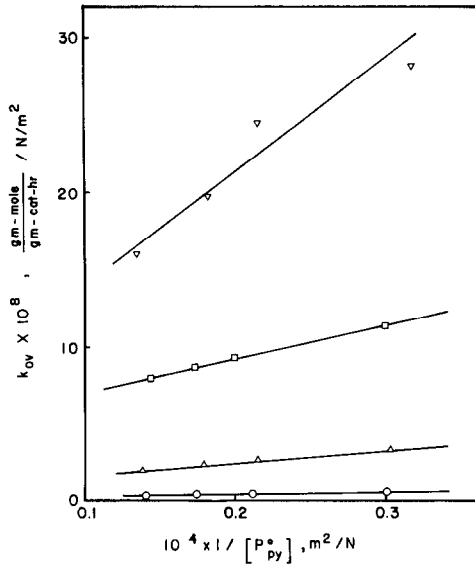


FIG. 5. Effect of  $[p_{py}^0]$  on overall constant,  $k_{ov}$ .  $[p_{py}^0]$ :  $\circ$ ,  $7.14 \times 10^4$ ;  $\Delta$ ,  $5.74 \times 10^4$ ;  $\square$ ,  $4.8 \times 10^4$ ;  $\nabla$ ,  $3.2 \times 10^4$  N/m<sup>2</sup>.

W/Al<sub>2</sub>O<sub>3</sub> catalyst proceeds through the following main reactions:

- (i) Saturation of the double bonds of pyridine and formation of piperidine.
- (ii) Disproportionation of piperidine to form ammonia and *n*-pentyl piperidine.
- (iii) Formation of *n*-pentane from *n*-pentyl piperidine.

The effect of feed composition upon the initial rate of reaction showed that adsorption of hydrogen is the rate-controlling step. The apparent rate constant was found inversely proportional to the initial pressure of pyridine.

The average activation energy was found to be 13.69 kcal/mole. The rate equation

TABLE I

Summary of Constants in The Rate Constant Expression  $k_{ov} = k_s/Wp_{py}^0] + k_i$

Temperature (°C)	$k_s \times 10^4$ moles/g.cat-hr	$k_i \times 10^8$ moles/g.cat-hr N/m <sup>2</sup>
145	1.6179	0.0337
195	7.6035	0.9576
245	22.4762	4.7484
280	74.7421	6.4522

for the hydrogenation of pyridine can be written as follows:

$$r = -\frac{d[p_{py}]}{dt} = \left( \frac{k_s}{[p_{py}^0]} + k_i \right) (p_{py})(p_{H_2})$$

ACKNOWLEDGMENT

The authors are grateful to the Department of Energy, Mines and Resources for financial assistance toward this project.

APPENDIX: NOMENCLATURE

- F* Flow rate of feed, moles/hr
- $k_i$  Reaction rate constant in a plot of  $k_{ov}$  vs  $1/[p_{py}^0]$ , mole/g.cat-hr (N/m<sup>2</sup>)
- $k_{ov}$  Observed rate constant for hydrogenation of pyridine, mole/g.cat-hr (N/m<sup>2</sup>)
- $k_s$  Reaction rate constant slope in a plot of  $k_{ov}$  vs  $1/[p_{py}^0]$ , mole/g.cat-hr
- $p_i$  Partial pressure of a component, N/m<sup>2</sup>.
- py* Pyridine
- r* Reaction rate, mole/g.cat-hr (N/m<sup>2</sup>)
- $\bar{R}$  Mole ratio of the feed (hydrogen/pyridine)
- t* *W/F*, time (g cat-hr/g mole)
- T* Temperature

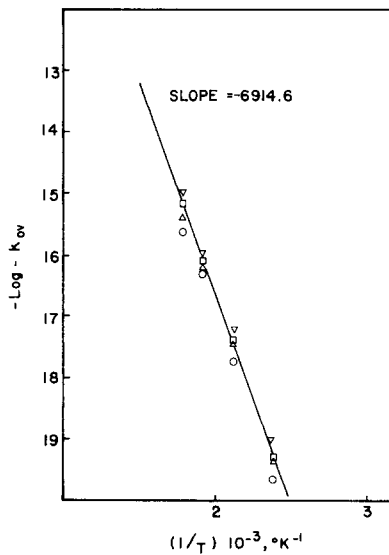


FIG. 6. Effect of temperature on rate constant at  $[p_{py}^0]$  =  $\circ$ ,  $7.14 \times 10^4$ ;  $\Delta$ ,  $5.74 \times 10^4$ ;  $\square$ ,  $4.8 \times 10^4$ ;  $\nabla$ ,  $3.2 \times 10^4$  N/m<sup>2</sup>.

W Weight of catalyst, g  
X Conversion of pyridine  
° Superscript, in the feed

## REFERENCES

1. Cox, K. E., Ph.D. Thesis, Montana State College, Bozeman, 1961.
2. Aboul-Gheit, A. K., Abdou, I. K., and Moustafa, A., *Egypt. J. Chem.* **17**(6), 853 (1974); **17**(5), 631 (1974).
3. Sonnemans, J., Vandenberg, G. H., and Mars, P., *J. Catal.* **31**, 220 (1973).
4. Bengeling, T., Boduszynski, M., Gourdiaan, F., and Sonnemans, J., *Anal. Lett.* **4**, 727 (1971).
5. Goudriaan, F., Ph.D. Thesis, Twent. Tech. Inst., The Netherlands, 1974.
6. McIlvried, H. G., *Ind. Eng. Chem. Proc. Res. Develop.* **10**(1), 125 (1971).
7. Satterfield, C. N., Model, M., and Mayer, J. F., *AIChE J.* **21**, 1100 (1975).
8. Sonnemans, J., Meyens, W. J., and Mars, P., *J. Catal.* **34**, 230 (1974).
9. Gupta, R. K., Mann, R. S., and Gupta, A. K., *J. Appl. Chem. Biotechnol.* **28**, 641 (1978).
10. Weisser, O., and Landa, S. "Sulphide Catalysts: Their Properties and Applications." Pergamon, New York, 1973.
11. Ng Kung, T., and Hercules, D. M., *J. Phys. Chem.* **80**, 2094 (1976).
12. Magnusson, H. W., and Schierz, E. R., *Univ. Wyo. Publ.* **7**, 1 (1940); *Chem. Abstr.* **34**, 6867.
13. Yoshida, F., Ramaswani, D., and Hougen, O. A., *AIChE J.* **8**, 5 (1962).